Published in "Physical Review B - Condensed matter and materials physics
85(19):195111 , 2012"
which should be cited to refer to this work.

Ab initio many-body effects in $TiSe_2$: A possible excitonic insulator scenario from GW band-shape renormalization

M. Cazzaniga,[1,2] H. Cercellier,[3] M. Holzmann,[4,2] C. Monney,[5] P. Aebi,[6] G. Onida,[1,2] and V. Olevano[3,2]
[1]*Università degli Studi di Milano, Physics Department, Milano, Italy*
[2]*European Theoretical Spectroscopy Facility (ETSF)*
[3]*Institut Néel, CNRS and UJF, Grenoble, France*
[4]*LPTMC, CNRS and UPMC, Paris and LPMMC, CNRS and UJF, Grenoble, France*
[5]*Synchrotron Radiation and Nanotechnology Department, Paul Scherrer Institut, Villigen, Switzerland*
[6]*Département de Physique and Fribourg Center for Nanomaterials, Université de Fribourg, Fribourg, Switzerland*

We present both theoretical *ab-initio* results within the Hedin's GW approximation and experimental angle-resolved photoemission and scanning tunneling spectroscopy measurements on $TiSe_2$. With respect to the density-functional Kohn-Sham metallic picture, the many-body GW self-energy leads to a ≈0.2-eV band-gap insulator consistent with our STS spectra at 5 K. The highest valence and the lowest conduction bands are strongly renormalized, with a loss of k^2 parabolic dispersion toward a k^4 shape. In particular, GW moves the top of valence moved toward a circle of points away from Γ, arising in a *Mexican hat* shape commonly associated with an *excitonic insulator*. Our calculations are in good agreement with experiment.

I. INTRODUCTION

Crystalline solids are classified as either insulators or metals, depending on the existence or absence of a finite energy gap in the electronic excitation spectrum. Within the independent particle picture, metallic or insulating behavior is explained in terms of partially or completely filled valence bands, but electronic correlations may overcome this ordinary paradigm and lead to new mechanisms for transforming a metal into an insulator or *vice versa*. From the early works of Mott, Kohn, and Hubbard,[1–3] several systems showing such exotic behavior have been supposed to exist in nature. One of them is the so-called *excitonic insulator*,[1,4–12] first predicted and in particular studied in the works of Mott, Kopaev, Keldysh, and Kohn and not to be confused with the more celebrated Mott-Hubbard insulator. Here we study the possibility of an excitonic insulator phase in titanium diselenide ($TiSe_2$)[13] based on *ab initio* many-body GW[14,15] theoretical results (Hedin's GW approximation), experimental photoemission spectra, and STS measurements.

At a noninteracting one-electron level, an excitonic insulator would present a semimetallic or semiconducting band structure with a sufficiently small (typically a few tens of millielectronvolts) overlap or gap and a reduced number of free carriers. Consequently, the Coulomb interaction between particles is only weakly screened. Electrons and holes can then spontaneously bind into nonconducting excitons and form a new ground state of lower energy than the normal phase. Exciton condensation may also lead to the formation of charge-density waves (CDWs) of purely electronic origin. On the semimetal side, model descriptions of the system are based on a BCS-like approach where the role of electron-electron Cooper pairs is taken by electron-hole excitons. Similar to BCS superconductors, an energy gap opens of the same order of magnitude as the binding energy of the pair[16] (depending on the underlying band structure, e.g., effective mass anisotropy and multivalley effects).

So far there is no clear-cut experimental proof of the excitonic insulator existence in nature. Nevertheless, several experimental observations point to $TiSe_2$ as one of the most probable candidates.[17–23] Indeed, a CDW has been observed in the ground state of $TiSe_2$, like in other transition-metal dichalcogenides, but so far, there is no consensus on the interpretation of the ground state and its CDW. In particular, the exact role played by excitons is still controversial. Either a Jahn-Teller effect[24,25] or a correlation mechanism leading to the excitonic insulator[18,19] has been invoked. Recently, it was suggested that the ground state and the resulting periodic lattice distortion (PLD) that occurs below 202 K are primarily due to electron-phonon coupling, which is only enhanced by the presence of incoherent excitons.[26] On the other hand, photoemission spectra are consistent with the excitonic insulator scenario,[20,23] and the interaction between an exciton condensate and phonons can reproduce the observed atomic displacements in the PLD with good agreement.[22]

In this work we provide theoretical evidence from *ab initio* many-body GW quasiparticle calculations supporting the excitonic insulator scenario in $TiSe_2$ and verify our calculations against angle-resolved photoemission spectroscopy (ARPES) measurements and scanning tunneling spectra (STS). STS at 5 K shows a band gap of ≃0.15 eV and points to $TiSe_2$ as a semiconductor. With respect to the one-electron mean-field density-functional theory (DFT) band structure, where $TiSe_2$ is a metal, the GW many-body self-energy opens a band gap of ≃0.2 eV, thus leading to an insulator. Furthermore, the band shape at high-symmetry points is strongly renormalized. In particular, the top of valence is moved from Γ toward a circle of points away from Γ, building up a *Mexican hat* feature characteristic of an excitonic insulator, as predicted by Kohn.[10] ARPES spectra indicate a flattening of the topmost valence bands before Γ, compatible with the Mexican hat picture. The GW bands we obtain are in good agreement with ARPES measurements, and also our STS spectra compare more favorably with the GW density of states (DOS) than with DFT.

The calculated dielectric function describing the screening properties of the system is in good agreement with previously measured energy-loss spectra (EELS).[27] The overall picture arising from our results indicates a possible ground-state instability in $TiSe_2$ of *electronic* origin. Furthermore, our calculations show that bare GW is able to reproduce the photoemission band structure of systems with strong excitonic renormalizations, although, in general, vertex corrections beyond GW are necessary to properly describe excitons in the optical spectra.[28]

II. THEORY

The calculations presented in this paper have been performed within the nonreconstructed primitive-hexagonal crystal structure ($P\bar{3}m1$). We consider separately the issue of a possible PLD, as discussed in Sec. VII. Our first step is a standard, numerically well converged[29] ground-state DFT local density approximation (LDA) calculation of the total energy, the electronic density, and the lattice parameters. The DFT calculation provides the Kohn-Sham (KS) electronic structure that we use for calculating the Green's function G and the dynamically screened interaction $W(\omega) = \varepsilon^{-1}(\omega)v$—defined as the bare Coulomb interaction v screened by the dynamical dielectric function $\varepsilon^{-1}(\omega)$—both entering into the self-energy in the GW approximation:[14,15]

$$\Sigma^{\mathrm{GW}}(r,r',\omega) = \frac{i}{2\pi}\int_{-\infty}^{\infty} d\omega'\, G(r,r',\omega-\omega')W(r,r',\omega').$$

Within a perturbative approach to first order in $\Sigma - v_{xc}^{\mathrm{LDA}}$ (with v_{xc}^{LDA} the LDA exchange-correlation potential), we calculate the GW quasiparticle energies, expanding Σ around the KS energies $\epsilon_{nk}^{\mathrm{KS}}$, taken as a zeroth-order approximation for the true quasiparticle energies,

$$\epsilon_{nk}^{\mathrm{GW}} = \epsilon_{nk}^{\mathrm{KS}} + Z\langle nk|\Sigma^{\mathrm{GW}}\left(\omega=\epsilon_{nk}^{\mathrm{KS}}\right) - v_{xc}^{\mathrm{LDA}}|nk\rangle,$$

where $Z = (1 - \partial\Sigma^{\mathrm{GW}}/\partial\omega|_{\omega=\epsilon_{nk}^{\mathrm{KS}}})^{-1}$.

In the standard GW approach, the dielectric function $\varepsilon^{-1}(\omega)$ is calculated in the RPA approximation.[30] Since screening is of crucial importance for exciton formation, we have checked the RPA energy-loss function $-\Im\varepsilon^{-1}(\omega)$ against the results of ellipsometry experiments[27] (see Fig. 1). From the good agreement with experiment, we are confident that the used RPA screening accurately describes the physical situation, but we have checked that our final results are not sensitive to the detailed features and are also obtained within a single plasmon-pole model. Notice that the effective screening of our *ab initio* RPA calculation is much weaker than the Lindhard[30] function used in the model calculation of Ref. 21, so that we expect that exciton formation is even more favored.[31,32]

III. EXPERIMENT

Photon-energy-dependent ARPES measurements were carried out at the SIS beamline of the Swiss Light Source synchrotron using a Scienta SES-2002 spectrometer with an overall energy resolution better than 10 meV and an angular resolution better than 0.5 deg. The data shown here have been collected at 65 K on two samples from the same batch with a slight Ti overdoping, resulting in a small population

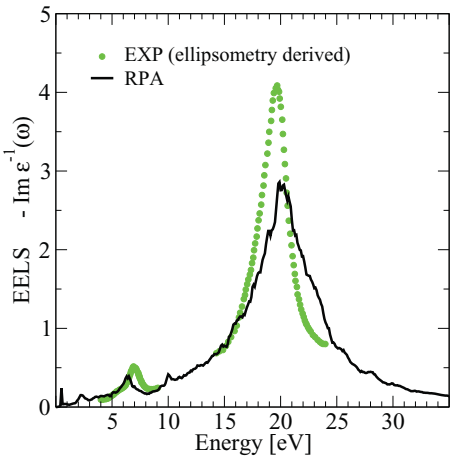

FIG. 1. (Color online) Energy-loss function. Green dots: experiment (Ref. 27) (derived from ellipsometry); black curve: present theoretical RPA result.

of the electron pocket at the L point and a consequent shift of the valence band. Scanning tunneling microscopy (STM) and spectroscopy (STS) measurements were performed on atomically flat and clean surfaces exhibiting the 2×2 CDW modulation (see Fig. 2). STS measurements were carried out in a OMICRON LT-STM microscope with use of the standard lock-in technique. Samples from the same batch were used for ARPES and STM/STS in order to compare the results of both experiments. The estimated energy resolution is about 10 meV.

IV. RESULTS: STS AND GW BAND GAP

The results of our STS measurements at 5 K are given in Fig. 2. We plot the differential conductance (dI/dV) as a function of the bias V. For small enough biases and slowly varying tunneling matrix elements, the differential conductance gives an image of the local density of states (DOS) that can be compared with calculations. At small bias the experimental dI/dV vanishes, indicating a gap of $\simeq$0.15 eV. With respect to the long-debated $TiSe_2$ semimetal-semiconductor question,[33] our STS spectra provide a *clear indication of*

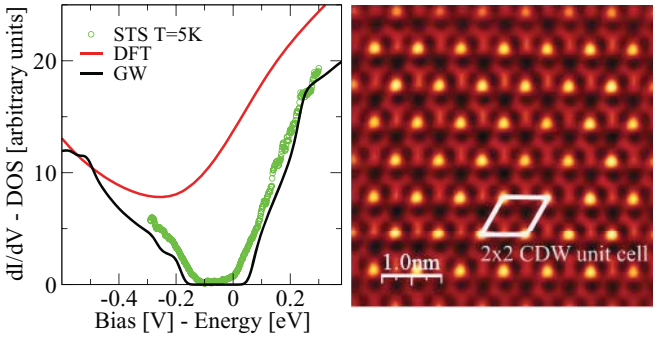

FIG. 2. (Color online) Left panel: STS dI/dV experimental spectra (green circles) vs GW (shifted to account for finite impurity doping of the sample, black curve) and DFT (zeroed at E_F, red curve) DOS for $TiSe_2$. Right panel: atomic resolution image of $TiSe_2$ at 77 K (tunneling parameters $V = -20$ mV and $I = 1.5$ nA).

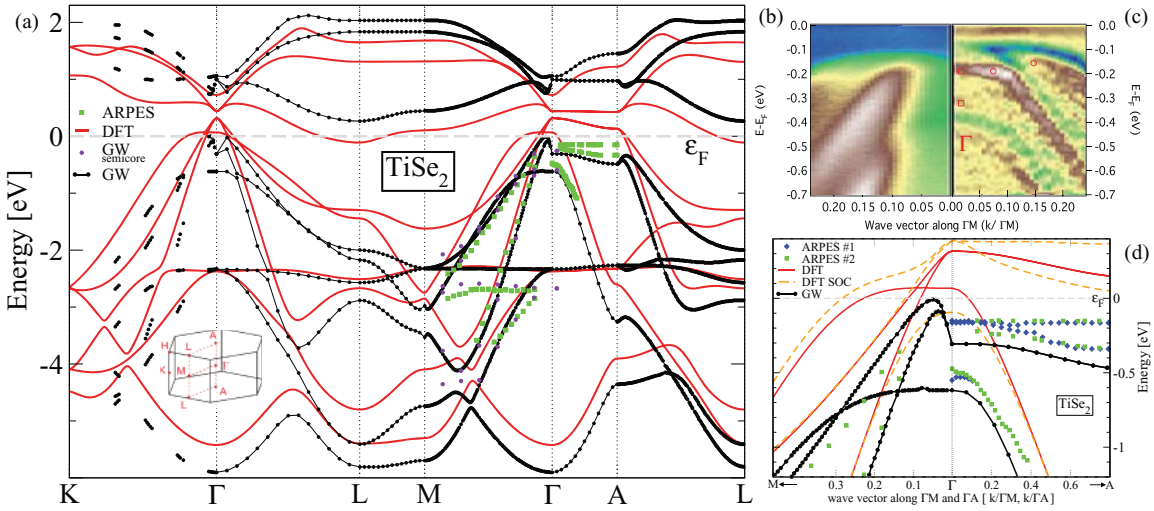

FIG. 3. (Color online) $TiSe_2$ band plot (panel a) and its zoom (d) at Γ (M-Γ-A directions). Red lines: DFT-LDA KS electronic structure; yellow dashed lines: DFT plus spin-orbit correction (SOC); black dots and lines: GW band plot; violet dots: GW results including Ti $3s3p$ electrons in valence; blue diamonds and green squares: samples 1 and 2 ARPES experimental data at $T = 65$ K. Panel b: ARPES signal $I(k,E)$; and c: its derivative d^2I/dE^2 taken at $T = 65$ K around Γ, *both* in the Γ-M direction.

semiconducting character, at least at low temperature. The STS gap is in quantitative agreement with recent ARPES experiments.[18,19,24,33,34] In Fig. 2 one can see that the calculated DFT DOS never vanishes, thus indicating a metal. On the other hand, the GW DOS presents a well-defined gap of 0.2 eV, slightly overestimated compared to STS. Contrary to DFT, GW predicts that $TiSe_2$ is a very small gap insulator, in agreement with the experiment. The left-valence and right-conduction DOS profiles are also well reproduced by GW.

V. RESULTS: THE BAND PLOT

In Fig. 3(a) we report the band plot of $TiSe_2$ based on DFT-LDA and GW calculations, together with experimental ARPES data. According to the DFT KS electronic structure, $TiSe_2$ is metallic with a band overlap of 0.4 eV between the top of the pocket of holes at Γ and the bottom of the pocket of electrons at L. The GW electronic structure then leads to a general shift of the bands, negative for the lowest and positive for the highest, and opens a band gap of around 0.2 eV. Therefore, many-body effects, as accounted by the GW approximation, turn the KS metal into a small gap insulator. As this is a common many-body effect, like, e.g., in germanium, it is not a novelty in itself. However, the *important modification of the band shape* shown in Fig. 3(d) is quite unusual: the top of valence is moved away from Γ, toward $k \simeq 0.05/\Gamma$M(K), where a band flattening, $d\epsilon/dk = 0$, occurs. This results in a loss of k^2 parabolic toward a k^4 *Mexican hat* shape. Similar reshaping also appears for the lowest two empty bands at Γ and at A, and, less pronounced, for two lower bands at A and M. Such Mexican hat features have been predicted by Kohn[10] to occur in excitonic phases. Our results provide an observation of this characteristic shape from *ab initio* GW calculations, pointing to an excitonic origin of the insulating nature of $TiSe_2$.

Our Fig. 3(b) and previous ARPES experiments[19,34] show a weakening of the signal in the neighborhood of Γ, so that the band structure cannot be clearly resolved there. However, Kidd *et al.* first remarked a loss of parabolic shape of the Se $4p$ band, together with a flattening [see Fig. 1(b) and text in Ref. 19] occurring at $k \simeq 0.05/\Gamma$K, which is confirmed also along ΓM by our ARPES spectra [Fig. 3(b)]. A plot of the second derivative d^2I/dE^2 of the ARPES signal [Fig. 3(c)] presents further anomalies: at Γ we observe a peak at $\simeq -0.5$ eV, to be interpreted as the light electron Γ_2^- band, and two peaks at $\simeq -0.3$ and $\simeq -0.2$ eV [red squares in Fig. 3(c)], probably corresponding to a split of the Γ_3^- Se $4p$ degenerate bands at Γ. Since those bands top at $E \simeq -0.2$ eV and at $E \simeq -0.15$ eV [red circles in Fig. 3(c)], we infer that a band bending should occur in order to achieve the lowest energies at Γ. Anyway, even in the case of a flatband interval as in the fit proposed by Kidd *et al.*, ARPES clearly indicates a departure from the k^2 parabolic toward a k^4 fourth-order polynomial, and this is in agreement with the GW band-shape renormalization.

For the rest of the band plot [Figs. 3(a) and 3(d)], experimental ARPES points agree much better with the GW band plot than with DFT KS, both in the ΓM and in ΓA directions. DFT presents empty Se $4p$ bands around Γ and along ΓA, giving rise to a pocket of holes at Γ. This is in striking contrast with ours [Fig. 3(b)] and all previous ARPES results[18–20,24,34] which found occupied Se $4p$ bands and no pocket of holes, exactly like in our GW calculation. Although the question was long debated, the most recent ARPES experiments[18,19,24,33–35] seem to indicate an indirect band gap of $\simeq$150 meV between the Se $4p$ bands at Γ and the "emerging" (above E_F and just only thermally occupied) Ti $3d$-derived band at L. This scenario is in good agreement with our GW band structure and in contrast with DFT[36] and the oldest ARPES experiments,[37–41] which rather found a band overlap. Residual mismatches of our GW and ARPES bands, like the split of the two Se $4p$ bands along ΓA, can be solved by including the spin-orbit coupling (SOC), as one can see by comparing DFT and DFT SOC bands in Fig. 3(d). SOC and relativistic corrections also have also important effects in band-crossing avoidance. Finally, the

mismatch in the position of the flat Ti $3d$ band at -2.5 eV is due to the lack of semicore electrons. Inclusion of semicore Ti $3s3p$ electrons into the pseudopotential valence shell [violet dots in Fig. 3(a)] improves the position of the $3d$ bands with respect to the experiment.

VI. MICROSCOPIC ANALYSIS OF THE MEXICAN HAT SCENARIO

In Fig. 4 we report the separate contributions of the diagonal matrix elements to the correlation $\langle nk|\Sigma_c^{\rm GW}|nk\rangle$ and exchange $\langle nk|\Sigma_x|nk\rangle$ self-energy, entering into the GW correction to the KS energies, for the three topmost occupied and the three lowermost empty states at Γ. It is evident that the Mexican hat renormalization is driven by exchange effects, not correlation. Bare exchange introduces changes of $\sim$2 eV between Γ and the new top-of-valence (TOV) circle of maxima (see the difference indicated by the arrow in Fig. 4), while screening effects included in the correlation part reduce this effect to a total value of around 0.3 eV. [See the difference between the TOV energy and the energy at Γ in Fig. 3(d).] Similar conclusions also hold for the two lowermost empty states at Γ, although with a softer renormalization.

Further study of the matrix elements of the electric dipole e^{-iqr} operator entering the exchange operator

$$\Sigma^x_{nk} = -\frac{4\pi}{V_{\rm BZ}} \sum_{n'k'} f_{n'k'} \frac{|\langle\psi_{n'k'}|e^{-i(k-k')r}|\psi_{nk}\rangle|^2}{|k'-k|^2} \qquad (1)$$

reveals that the Mexican hat shape for the four bands at Γ is mostly conjured by exchange with states on bands $n' =$ Se $4p_{3/2}$ and $4p_{1/2}$ at k' close to the Brillouin zone center and rather in the k_xk_y plane (we checked the ΓM direction). On the other hand, we have found that the contributions to the self-energy coming from exchange with states at k' along the k_z direction (ΓA direction) are negligible, like those from states faraway from Γ, e.g., the Brillouin zone boundary. The latter are suppressed by the $|k'-k|^2$ factor at the denominator in Eq. (1), although matrix elements at the numerator can be large. This analysis also indicates that the Mexican hat feature of our G_0W_0 is robust against self-consistent calculations. Indeed,

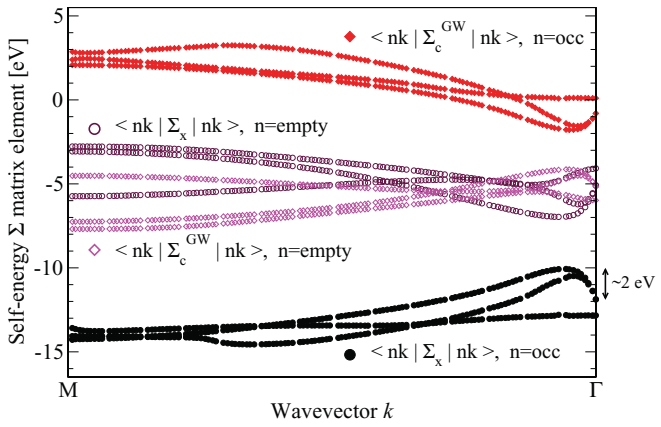

FIG. 4. (Color online) Exchange $\langle nk|\Sigma_x|nk\rangle$ (black circles) and correlation $\langle nk|\Sigma_c^{\rm GW}|nk\rangle$ (red diamonds) real part contributions to the self-energy matrix elements, for the three topmost occupied (filled symbols) and three lowest empty (empty symbols) bands along M-Γ.

the Ti $3d$-derived band, which is partially filled in DFT and becomes empty in GW, plays no role in the renormalization. In the next iterations the increased population of the Se $4p$ bands, mostly responsible for the renormalization, and the opening of a band gap, resulting in a reduction of the electron-hole screening, should further strengthen the renormalization, or at most not change the picture.

VII. DISCUSSION

Supposing that a realization of an excitonic insulator really exists in nature, the first question one may ask is whether the GW approximation is already sufficient to describe its quasiparticle electronic structure as sampled by ARPES, or whether vertex corrections beyond the GW approximation are needed. It is well known that vertex corrections, e.g., within the Bethe-Salpeter equation approach,[28] are required to properly describe excitons and the spectrum of *neutral* excitations as in optical absorption. However, in contrast to optical absorption, ARPES measures *charged* excitations. In the optical absorption case the focus is on the polarizability. An RPA approximation on the polarizability, even built on top of GW renormalized Green's functions, takes into account only bubble diagrams and neglects electron-hole interaction diagrams. Excitons, and more generally, excitonic effects in the neutral excitations spectrum, as sampled by optical absorption, cannot be described by a GW-RPA approximation, and vertex corrections to the bubble into the polarizability must be taken into account.

On the other hand, in the case of charged electron addition/removal excitations and ARPES, the focus is on the self-energy. A Feynman diagram expansion of the GW Green's function would show that hole (electron) channels are taken into account by the GW renormalization of the electron (hole) propagator toward quasiparticles. Bare electrons (holes) are dressed by virtual holes (electrons) introduced by the GW self-energy so that excitonic contributions, necessary to describe the quasiparticle excitation spectrum of an excitonic insulator, are already described at the level of the GW approximation.

Notice that these diagrams are already taken into account also at the level of bare or statically screened exchange, as e.g., in a Hartree-Fock approximation. This is clearly shown by our analysis reported in Fig. 4. In fact, the first seminal works[6,10,11] on the excitonic insulator were model studies, at best at the level of a statically screened Hartree-Fock approximation. Moreover, an important question that one may be asking is would the excitonic insulator physics resist a more realistic screening, like, e.g., in the GW approximation, or would this physics rather be swept away when a realistic screening between electrons and holes, as in a real material, i.e., a good candidate to an excitonic insulator, is taken into account? In the latter case, the excitonic insulator would remain a model construction, with no implementations in nature. The answer this work offers to this question, at the example of $TiSe_2$, is that GW *can* indeed describe the physics of an excitonic insulator. That is, the picture that emerged in the HF seminal works *resists* the inclusion of more correlation such as in GW. As we have seen in Fig. 4, the effect is strongly reduced by correlations, but it is still present. A realistic *ab initio* screening between electrons and holes, entering into the GW self-energy through the W factor, is not so effective to completely damp the

electron-hole interaction. Of course, this is a conclusion at the level of the GW approximation. We can't conclude whether the excitonic insulator picture would also resist introduction of vertex corrections beyond the GW approximation and toward the exact self-energy. However, at the GW level, one can rely on the validity of an approximation that, contrary to HF, has already provided broad statistics[42,43] of band gaps and band plots in good agreement with ARPES.

Let us now discuss whether the Mexican hat band renormalization provided by GW can be an indication of an excitonic insulator physics in $TiSe_2$. In fact, a Mexican hat renormalization of the band shape is typical of an excitonic phase, as Kohn has clearly shown,[10] and it was already contained in Eqs. (26) and (27) in the Keldysh and Kopaev paper,[6]

$$\epsilon^{\mathrm{QP}}_{c,v}(k) = \frac{\epsilon_c(k) + \epsilon_v(k)}{2} \pm \sqrt{\frac{(\epsilon_c(k) - \epsilon_v(k))^2}{4} + |\Delta(k)|^2}, \tag{2}$$

providing the quasiparticle (QP) renormalized conduction ϵ^{QP}_c and valence ϵ^{QP}_v bands, starting from noninteracting conduction and valence bands ϵ_c and ϵ_v, with $\Delta(k)$ representing the excitonic effect brought by the self-energy. Equation (2) is the result of a simplified self-energy calculation on a model containing only two bands. $\Delta(k)$ may be assumed independent of k in the energy region we are interested in, and with a constant Δ Eq. (2) provides the scenario represented in Fig. 5. We show the starting noninteracting parabolic bands, $\epsilon_{c,v}(k) = \pm k^2/2m^*_{c,v} \mp 1$, and the quasiparticle excitonic renormalized bands $\epsilon^{\mathrm{QP}}_{c,v}(k)$. One can see a departure from the parabolic k^2 behavior toward a typical Mexican hat band shape. By playing with the effective masses m^*_c, m^*_v and the self-energy strength Δ, one can explore different situations. Among them (right panel) is a situation where one of the bands appears flattened

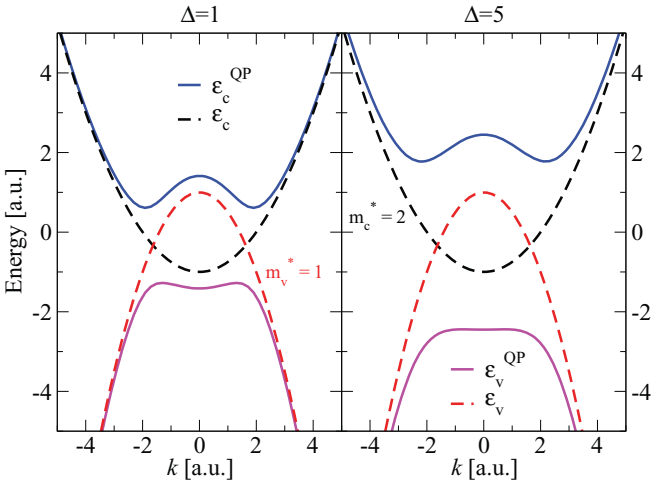

FIG. 5. (Color online) Scheme representing the renormalization of a noninteracting standard parabolic-bands metal into a Mexican-hat-shaped band excitonic insulator. Dashed lines: noninteracting conduction (black) and valence (red) metal overlapping bands, assuming the effective mass of electrons twice that of holes. Solid lines: excitonic insulator conduction (blue) and valence (magenta) Mexican-hat-shaped bands. For the left panel $\Delta = 1$, while for the right $\Delta = 5$. The plot is in arbitrary units.

rather than building up a Mexican hat shape, more similar to what $TiSe_2$ ARPES data on the Se $4p$ band at Γ seems to indicate.

A realistic description is of course much more complex than in the simple model here reported. More than two bands may enter into play, each one with different effective masses and anisotropic dispersions[16,20,44] and with different interaction between them.

The present GW calculation on $TiSe_2$ finds a Mexican hat many-body renormalization of quasiparticle energies very much like that presented by the simple self-energy model calculation Eq. (2) and Fig. 5. Notice that this was found by an *ab initio* calculation, without conjectures or adjustable parameters. The analysis of the GW matrix elements presented in the previous section has shown that strong electron-hole mixing is at the origin of this band-shape renormalization and supports the interpretation of $TiSe_2$ as a system presenting the physics of an excitonic insulator. As a necessary consequence, the system should present an instability of the normal ground state toward the spontaneous formation of excitons. From our *ab initio* GW calculations we cannot conclude whether excitons may form a condensate below a critical temperature and give rise to a CDW. This in its turn might induce a distortion of the atomic structure. Here, we have not further explored this instability.

It is important that this instability is emerging without invoking ionic degrees of freedom and from the side of a calculation on the nonreconstructed higher-symmetry atomic structure. This allows us to conclude that the mechanism acting in $TiSe_2$ is of purely electronic origin, without the necessity of a phonon-driven ionic mechanism.

It would be interesting to study the possibility of a CDW in $TiSe_2$ from calculations of the full GW Green's function in real space on the supercell. To address the possibility of a PLD, the coupling with the ionic degrees of freedom should be included within a self-consistent GW molecular dynamics driven by the minimization of the GW total energy and forces. This cannot change the electron-hole mixing and the excitonic instability scenario that emerged from this GW calculation at the undistorted atomic structure working point. However, there can be quantitative adjustments toward a better agreement with the observed experimental situation. A CDW would induce a $2 \times 2 \times 2$ superperiodicity and a folding of the Brillouin zone, so that the L point maps onto the Γ point. As a consequence, electron-hole mixing between the Ti $3d$ lowest conduction band and the Se $4p$ bands may occur, as the matrix elements are not any more damped by the $1/|k - k'|^2$ factor after the k-point folding. Also the Ti $3d$ band might be found to present a Mexican hat renormalization, like Kidd *et al.*[19] have found and which we have not found in the GW calculation here, while the Mexican hat renormalization of the Se $4p$ band might be reduced rather toward a flattening, like at least it seems an experimentally safe finding from our ARPES data and that of Ref. 19. So the question about the nonquantitative agreement between this GW calculation and the ARPES data on the Mexican hat or flattening is not well posed, because theory and experiment are not performed at the same working point. In both GW and ARPES we do observe a very well-defined departure from a k^2 dispersion toward a k^4 shape, which in fact have the same underlying excitonic physics, as the simple model Eq. (2) and Fig. 5 show.

VIII. CONCLUSIONS

We presented both theoretical GW and experimental ARPES and STS results on $TiSe_2$. The many-body GW self-energy opens a band gap of ≈0.2 eV and strongly renormalizes the band shape with the top of valence moved away from Γ toward a k^4 *Mexican hat* feature typical of an excitonic insulator. The calculations are in good agreement with EELS experiments and our STS and ARPES data, which clearly indicate a band gap and a departure from the k^2 band shape. Our calculation shows that the Mexican hat band renormalization is already present for the higher-symmetry nondistorted atomic structure and without invoking the role of ionic degrees of freedom. Analysis of the effect shows that the band-shape renormalization derives from a strong electron-hole mixing and supports the interpretation of $TiSe_2$ as a system presenting the physics of an excitonic insulator.

ACKNOWLEDGMENTS

We thank M. Gatti for useful discussions. P.A. acknowledges support by the Fonds National Suisse pour la Recherche Scientifique through Div. II and MaNEP. The high-resolution ARPES measurements were performed at the Surface and Interface Spectroscopy Beamline at the Swiss Light Source, Paul Scherrer Institute, Switzerland. We acknowledge Cineca for computer time and the RTRA NanoSTAR and ETSF for support.

[1] N. F. Mott, Philos. Mag. **6**, 287 (1961).
[2] W. Kohn, Phys. Rev. **133**, A171 (1964).
[3] J. Hubbard, Proc. R. Soc. London, Ser. A **277**, 237 (1964).
[4] R. G. Arkhipov, Zh. Eksp. Teor. Fiz. **43**, 349 (1962) [Sov. Phys. JETP **16**, 251 (1962)].
[5] R. S. Knox, in *Solid State Physics*, edited by F. Seitz and D. Turnbull (Academic, New York, 1963), Suppl. 5, p. 100.
[6] L. V. Keldysh and Y. V. Kopaev, Fiz. Tverd. Tela **6**, 2791 (1964) [Sov. Phys. Solid State **6**, 2219 (1965)].
[7] W. Kohn, in *Physics of Solids at High Pressures*, edited by C. T. Temiznka and R. M. Emrick (Academic, New York, 1965).
[8] A. N. Kozlov and L. A. Maksimov, Zh. Eksp. Teor. Fiz. **48**, 1184 (1965) [Sov. Phys. JETP **21**, 790 (1965)]; Zh. Eksp. Teor. Fiz. **49**, 1284 (1965) [Sov. Phys. JETP **22**, 889 (1966)].
[9] J. Des Cloizeaux, J. Phys. Chem. Solids **26**, 259 (1965).
[10] W. Kohn, Phys. Rev. Lett. **19**, 439 (1967).
[11] D. Jérome, T. M. Rice, and W. Kohn, Phys. Rev. **158**, 462 (1967).
[12] B. I. Halperin and T. M. Rice, Rev. Mod. Phys. **40**, 755 (1968), and references therein.
[13] J. A. Wilson and S. Mahajan, Comm. Phys. **2**, 23 (1977).
[14] L. Hedin, Phys. Rev. **139**, A796 (1965).
[15] G. Strinati, H. J. Mattausch, and W. Hanke, Phys. Rev. Lett. **45**, 290 (1980); Phys. Rev. B **25**, 2867 (1982).
[16] J. Zittartz, Phys. Rev. **162**, 752 (1967); **164**, 575 (1967); **165**, 605 (1968); **165**, 612 (1968).
[17] F. J. Di Salvo, D. E. Moncton, and J. V. Waszczak, Phys. Rev. B **14**, 4321 (1976).
[18] T. Pillo, J. Hayoz, H. Berger, F. Levy, L. Schlapbach, and P. Aebi, Phys. Rev. B **61**, 16213 (2000).
[19] T. E. Kidd, T. Miller, M. Y. Chou, and T. C. Chiang, Phys. Rev. Lett. **88**, 226402 (2002).
[20] H. Cercellier, C. Monney, F. Clerc, C. Battaglia, L. Despont, M. G. Garnier, H. Beck, P. Aebi, L. Patthey, H. Berger *et al.*, Phys. Rev. Lett. **99**, 146403 (2007).
[21] C. Monney, H. Cercellier, F. Clerc, C. Battaglia, E. F. Schwier, C. Didiot, M. G. Garnier, H. Beck, P. Aebi, H. Berger *et al.*, Phys. Rev. B **79**, 045116 (2009).
[22] C. Monney, C. Battaglia, H. Cercellier, P. Aebi, and H. Beck, Phys. Rev. Lett. **106**, 106404 (2011).
[23] T. Rohwer, S. Hellmann, M. Wiesenmayer, C. Sohrt, A. Stange, B. Slomski, A. Carr, Y. Liu, L. M. Avila, M. Kalläne *et al.*, Nature (London) **471**, 490 (2011).
[24] K. Rossnagel, L. Kipp, and M. Skibowski, Phys. Rev. B **65**, 235101 (2002).
[25] H. P. Hughes, J. Phys. C **10**, L319 (1977).
[26] J. van Wezel, P. Nahai-Williamson, and S. S. Saxena, Phys. Rev. B **83**, 024502 (2011).
[27] T. Buslaps, R. L. Johnson, and G. Jungk, Thin Solid Films **234**, 549 (1993).
[28] S. Albrecht, L. Reining, R. DelSole, and G. Onida, Phys. Rev. Lett. **80**, 4510 (1998); S. Albrecht, L. Reining, G. Onida, V. Olevano, and R. DelSole, *ibid.* **83**, 3971 (1999).
[29] We used the ABINIT code to perform DFT-LDA and GW pseudopotential calculations on a plane-wave basis. We used a Martins-Trouiller pseudopotential with an energy cutoff of 40 Ha on a $14 \times 14 \times 14$ k-point grid for the DFT calculations. For the GW calculation we used a series of ten 1/140 shifted grids, a cutoff of 32.8 Ha for wave functions, and 2.5 Ha for dielectric and self-energy matrix elements, and we included 80, 160 bands into screening and self-energy, respectively.
[30] J. Lindhard, Mat. Fys. Medd. K. Dan. Vidensk. Selsk. **28**, 8 (1954).
[31] R. Del Sole, G. Adragna, V. Olevano, and L. Reining, Phys. Rev. B **67**, 045207 (2003).
[32] H. C. Weissker, J. Serrano, S. Huotari, F. Bruneval, F. Sottile, G. Monaco, M. Krisch, V. Olevano, and L. Reining, Phys. Rev. Lett. **97**, 237602 (2006).
[33] J. C. E. Rasch, T. Stemmler, B. Muller, L. Dudy, and R. Manzke, Phys. Rev. Lett. **101**, 237602 (2008).
[34] D. Qian, D. Hsieh, L. Wray, E. Morosan, N. L. Wang, Y. Xia, R. J. Cava, and M. Z. Hasan, Phys. Rev. Lett. **98**, 117007 (2007).
[35] N. G. Stoffel, S. D. Kevan, and N. V. Smith, Phys. Rev. B **31**, 8049 (1985).
[36] A. Zunger and A. J. Freeman, Phys. Rev. B **17**, 1839 (1978).
[37] R. Z. Bachrach, M. Skibowski, and F. C. Brown, Phys. Rev. Lett. **37**, 40 (1976).
[38] M. M. Traum, G. Margaritondo, N. V. Smith, J. E. Rowe, and F. J. Di Salvo, Phys. Rev. B **17**, 1836 (1978).
[39] A. Galdikas, V. Jasutis, S. Kačiulis, G. Mattogno, A. Mironas, V. Olevano, D. Senulienė, and A. Šetkus, Sens. Act. B **43**, 140 (1997).
[40] C. H. Chen, W. Fabian, F. C. Brown, K. C. Woo, B. Davies, B. DeLong, and A. H. Thompson, Phys. Rev. B **21**, 615 (1980).
[41] O. Anderson, R. Manzke, and M. Skibowski, Phys. Rev. Lett. **55**, 2188 (1985).
[42] L. Hedin, J. Phys.: Condens. Matter **11**, R849 (1999).
[43] W. G. Aulbur, L. Jönsson, and J. W. Wilkins, Solid State Phys. **54**, 1 (1999).
[44] S. Botti, N. Vast, L. Reining, V. Olevano, and L. C. Andreani, Phys. Rev. Lett. **89**, 216803 (2002).